International Journal of Thin Films Science and Technology

http://dx.doi.org/10.18576/ijtfst/050103

Structural, Morphological, Optical and Electrical Properties of Spray Deposited Ternary CdZns Thin Films

V. Narasimman, V. S. Nagarethinam, K. Usharani and A. R. Balu[*].

PG and Research Department of Physics, AVVM Sri Pushpam College, Poondi – 613 503, Tamilnadu, India.

Received: 21 Aug. 2015, Revised: 2 Oct. 2015, Accepted: 10 Oct. 2015.
Published online: 1 Jan.2016.

Abstract: Nanostructured ternary CdZnS thin films with zinc concentrations (0, 2, 4, 6 and 8 wt.%) were prepared by spray pyrolysis technique using perfume atomizer on glass substrates at 400° C. The effect of Zn doping on the structural morphological, optical and electrical properties of the films was studied. All the films exhibit hexagonal structure with a preferential orientation along the (0 0 2) plane irrespective of the Zn doping level. SEM analysis showed that the film morphology modifies from clustered grains to nanosized needle shaped grains with Zn doping. Film transparency increases with Zn doping and the film coated with 6 wt.% Zn concentration exhibit a maximum transmittance of nearly 90% in the visible region. Optical band gap was blue shifted with increase in Zn doping which is associated with Moss-Burstein (MB) effect. PL and Raman spectra implied that more defects existed in the doped samples. All the films have resistivity in the order of 10^1 Ω-m and the CdS film coated with 6 wt.% Zn concentration had a minimum resistivity of 0.675 x 10^1 Ω-m.

Keywords:X-ray diffraction; thin films; crystal structure; texture coefficient; optical band gap.

1 Introduction

Cadmium sulphide (CdS) is an II-VI compound semiconductor which play an important role in visible-light-driven optoelectronic applications because of its wide energy band gap (2.42 eV), high electron affinity and n-type conductivity. CdS thin films grow usually in the wurtzite structure and without external doping show n-type conductivity, which might be due to native defects or sulphur vacancies and cadmium interstitials. Due to its wide and direct band gap transition, high refractive index (2.5) and high electron affinity, CdS is known to be an excellent heterojunction partner for p-type CdTe, p-type Cu(In)Se_2 solar cells. It has been widely used as a window material in high efficiency thin film solar cells based on CdTe or Cu(In) Se_2 and in photoelectrochemical solar cells [1-3].

However, the polycrystalline CdS, when used in solar cells, has some adverse properties arising from the low band gap, thickness and lattice mismatch, which create high defect density [4]. To enhance the performance of CdS as an efficient window material for solar cell applications several properties are required: (i) relatively high transparency (ii) not too thick to favour absorption or thin to avoid short circuiting. (iii) Very high conductivity to reduce solar cell electrical losses and higher photoconductivity not to alter the solar cell spectral response. It is well known that impurities in semiconductors often cause dramatic changes in their structural, electrical and optical properties. It has been reported earlier that doping CdS with elements such as indium (In^{3+}) [5], aluminium (Al^{3+}) [6], gallium (Ga^{3+}) [7], Boron (B^{3+}) [8], Manganese Mn^{2+} [9], iron (Fe^{2+}) [10] can enhance its optical, electrical and magnetic properties. Zinc Sulphide (ZnS) is a promising material for its application as window and buffer layers in thin solar cells, due to its good transparency in the visible region.

As mentioned earlier, CdS thin films are typically n-type, with relatively low resistivity depending upon the growth conditions, while ZnS thin film usually have very low resistivity with a band gap around 3.5 to 3.7 eV [11]. Hence it is expected that the homogenous composing of these two materials allow intermediate optical and electrical properties between those of pure CdS and ZnS, making it attractive for various applications such as window layers on solar cells. Zinc is an important transition metal element having an ionic radius of 0.074 nm which is smaller than that of Cd^{2+} (0.097 nm) and hence Zn^{2+} can easily penetrate into CdS crystal lattice replacing Cd^{2+} ions, improving its physical properties. The equal valencies and close electro negativities (1.7 and 1.6 Pauling for Cd and Zn,

[*]Corresponding author E-mail: arbalu757@gmail.com

respectively) also favours for the substitution of Zn^{2+} into CdS lattice.

Accommodation of wide range of Zn into the CdS lattice can tune its energy band gap and improve its electrical properties. So in the present work CdZnS thin films were fabricated by spray pyrolysis technique with different Zn concentrations (0, 2, 4, 6, and 8 wt.%) and the effect of Zn doping on the structural, morphological, optical and electrical properties of CdS thin films was investigated. The use of perfume atomizer has many advantages over the conventional spray technique such as: no need for carrier gas, fine atomization and enhanced wettability between sprayed micro particles and the previously deposited layers [12].

2 Experimental Details

The undoped CdS and Zn-doped CdS (CdZnS) thin films were deposited by spray pyrolysis technique using a perfume atomizer. Chemicals used for the deposition of CdS and CdS:Zn films were cadmium chlorine, thiourea and zinc chloride. All the chemicals were of analytical reagent grade (sigma make, with a purity of 99.9%). The deposition of CdS thin films was performed on ultrasonically cleaned glass substrates (micro slides of dimensions 76 x 25 x 1.5 mm^3) kept at 400°c by spraying an aqueous solution (50 ml in volume) containing 0.1M of cadmium chloride and thiourea. $ZnCl_2$ with different concentrations (0, 2, 4, 6 and 8 wt %) were added to the starting solution for Zn doping.

3 Results and Discussion

3.1 Structural studies

The X-ray diffraction patterns of Zn-doped CdS thin films deposited with different Zn concentrations (0, 2, 4, 6 and 8 wt. %) in the starting solution are shown in Figure 1.

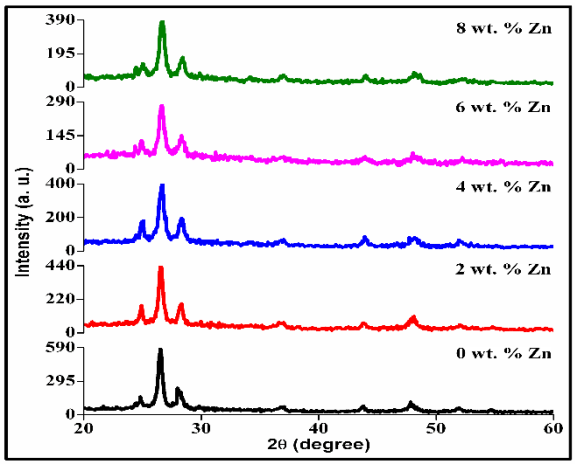

Figure1: XRD patterns of CdZnS thin film.

From the patterns it is clear that the films are polycrystalline in nature. The peaks observed from the diffraction patterns at 2θ = 24.79°, 26.497°, 28.15°, 36.78°, 43.72°, 47.83° and 51.9° are characteristic of pure CdS, suggesting that incorporation of Zn in the films does not imply changes in the crystalline phase of CdS. The peaks were indexed to (1 0 0), (0 0 2), (1 0 1), (1 0 2), (1 1 0), (1 0 3) and (1 1 2) planes of pure CdS (JCPDS card No. 41-1049). A matching of the calculated d_{hkl} values and the standard ones (Table 1) confirmed that all the deposited films (undoped and Zn-doped CdS) are crystallised in the hexagonal structure with a preferred orientation of the crystallites along the (0 0 2) direction such that the c-axis is perpendicular to the surface of the substrate. The preferential orientation along the (0 0 2) plane observed here exactly matches with the results reported by Sivaraman et al. [13] for Mg-doped CdS thin films fabricated using perfume atomizer.

The preferential orientation of the Zn doped CdS thin films are evaluated by the texture coefficient (TC), calculated from the X-ray data using the formula [14]:

$$TC(hkl) = \frac{I\,(hkl)/I_0(hkl)}{N^{-1}\sum I\,(hkl)/\,I_0(hkl)} \qquad (1)$$

Where I(h k l) is the measured intensity of the (h k l) plane, I_o(h k l) is the corresponding standard intensity of the (h k l) and N is the number of reflections. Figure 2 represents TC(h k l) values calculated for the reflections (1 0 0), (0 0 2), (1 0 1) (1 1 0) and (1 0 3) of the hexagonal Zn-doped CdS at the examined Zn doping range.

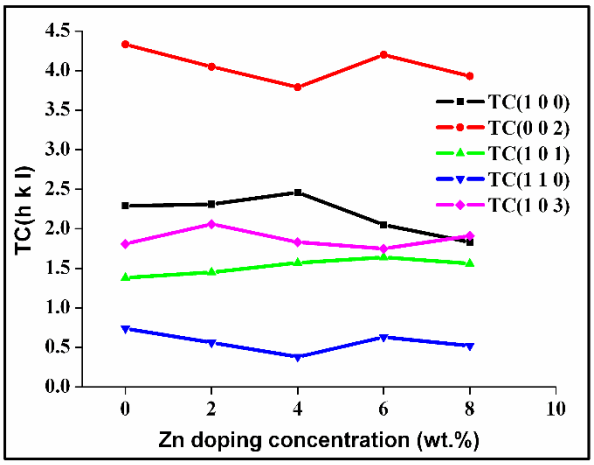

Figure 2: Variation of texture of coefficient values of CdZnS thin films

It can be seen that all the Zn-doped CdS films exhibited larger TC value for the (0 0 2) plane, indicating that the doped films had a c-axis preferred orientation. The lattice parameter 'a' and 'c' calculated from the position of the XRD (0 0 2) peak are presented in Table 2. It can be observed that the lattice parameter values decreases with Zn doping, which confirms that incorporation of Zn^{2+} into the CdS lattice decreases the lattice volume. Since the ionic radius of Cd^{2+} (0.97Å) is greater than that of Zn^{2+} (0.74Å),

the decrease in the lattice volume can be attributed to substitutional incorporation of Zn^{2+} ions instead of Cd^{2+} ions. The shift in the 2θ value of the (0 0 2) peak towards higher angle (Table 2) strongly favours for this supposition.

The crystallite sizes (D) of the CdZnS films was calculated by using the Scherrer relation [15]:

Table 1: Comparison of standard and observed'd' spacing values of CdZnS thin films

(h k l)	d-spacing*	Observed 'd' (Å) Zinc concentration (wt. %)				
		0	2	4	6	8
(1 0 0)	3.5861	3.5881	3.5776	3.5681	3.5726	3.5584
(0 0 2)	3.3599	3.3612	3.3555	3.3481	3.3471	3.3498
(1 0 1)	3.1638	3.1678	3.1572	3.1502	3.1507	3.1440
(1 0 2)	2.4519	2.4417	2.4448	2.4386	2.4386	2.4308
(1 1 0)	2.0705	2.0690	2.0636	2.0598	2.0609	2.0572
(1 0 3)	1.8998	1.9002	1.8949	1.8911	1.8866	1.8869
(1 1 2)	1.7627	1.7605	1.7572	1.7559	1.7505	1.7511

*JCPDS card No. 41-1049

Table 2: Structural parameters of CdZnS thin films

Zn doping concentration (wt.%)	$2\theta_{(0\,0\,2)}$	Crystallite size (nm)		Strain ε x10^{-3}	Lattice parameters		
		Scherrer formula	From W-H plots		a* (Å)	c*(Å)	c/a
0	26.5°	20.40	28.57	1.7	4.117	6.722	1.6327
2	26.542°	19.91	25.77	1.741	4.110	6.711	1.6328
4	26.602°	18.14	23.26	1.911	4.101	6.696	1.6328
6	26.645°	16.35	18.52	1.953	4.099	6.694	1.6331
8	26.610°	17.75	19.61	2.123	4.094	6.686	1.6331

$$D = \frac{0.9\,\lambda}{\beta \cos\theta} \quad (2)$$

where β is the full width at half maximum (FWHM), λ is the wavelength of the X-ray (1.5406 Å) and θ is the angle of diffraction. The crystallite size was also calculated using the Willamson–Hall (W-H) method according to the relation [16]:

$$\frac{\beta\, cos\theta}{\lambda} = \frac{1}{D} + \frac{\varepsilon\, sin\theta}{\lambda} \quad (3)$$

The crystallite size value was determined from the reciprocal of the intercept on the y-axis of plot between β cosθ/λ and sinθ/λ (Figure 3).

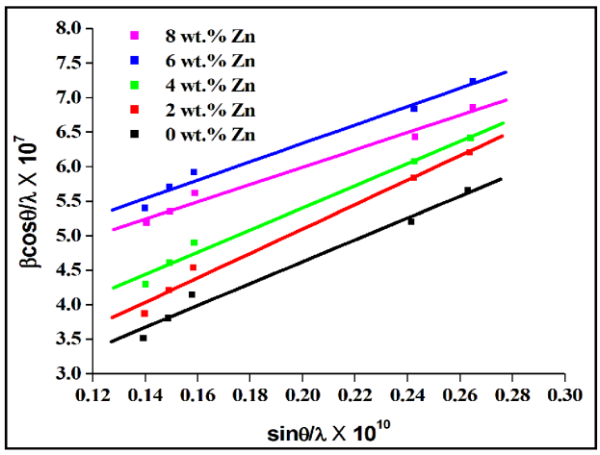

Figure 3: W-H plots of CdZns thin films.

The crystallite size values calculated using the Scherrer relation and from the W-H plots are compiled in Table 2. It is observed that the crystallite size values decreases with increasing Zn content in the films as expected since the ionic radius of Zn is smaller than that of Cd. Micro strain is calculated by the formula $\boldsymbol{\varepsilon = \frac{\beta\, cos\theta}{4}}$ as reported by Balu et al. [17] and the calculated values are compiled in Table 2. It is observed that strain is enhanced with Zn incorporation. Because of lattice contraction, strain is increased and it results in decrease in crystallite size values of the doped films.

3.2 SEM and elemental analysis

Figure 4 (a - e) shows the SEM images of CdZnS thin films coated with different Zn concentrations. The SEM micrograph of undoped CdS thin film (Figure 4(a)) reveals compact surface with nanosized grains interconnected with each other. With increase in Zn concentration, the film surface modifies with clouds of grains appearing almost throughout the entire surface for the film coated with 2 wt.% Zn concentration (Figure 4(b)). No cloudy appearance is visible for the CdZnS film coated with 4 wt.% Zn concentration and the surface appears smooth with fully covered nano sized grains of unequal sizes (Figure 4(c)). With further increase in Zn concentration, the surface modifies with equally sized nano grains scattered throughout the entire film surface for the CdZnS film with 6 wt.% doping concentration (Figure 4(e)). For the film coated with 8 wt.% Zn doping concentration, needle shaped grains are evinced (Figure 4(e)). Few pinholes and cracks are also visible. These results infer that the CdS film morphology changer from interconnected grain nature to loosely bounded nano needles with Zn doping.

The composition of Zn-doped CdS thin films were confirmed by energy dispersive X-ray spectroscopy (EDAX). The representative EDAX spectra of the undoped and 6 wt.% Zn doped CdS thin films are shown in Figure 5.

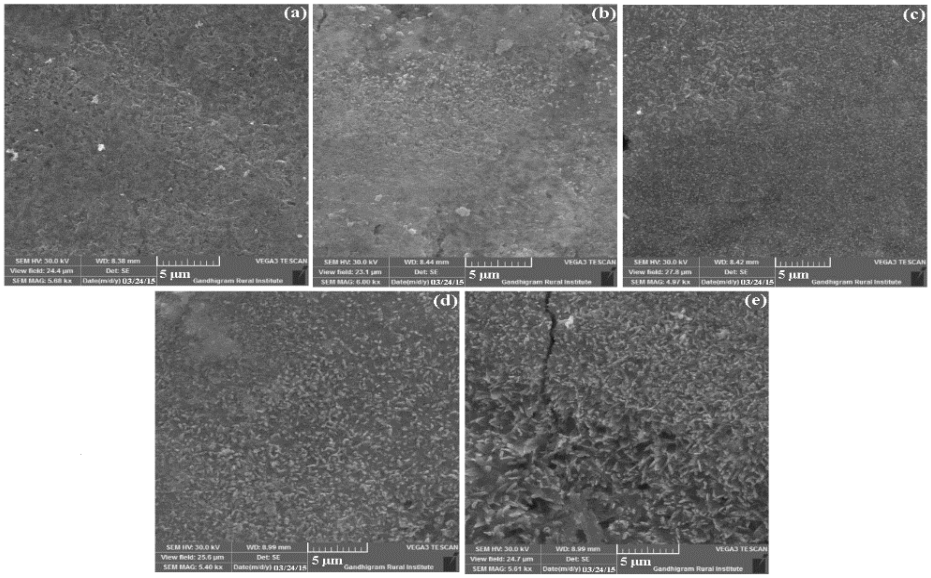

Figure 4: SEM images of CdZnS thin films

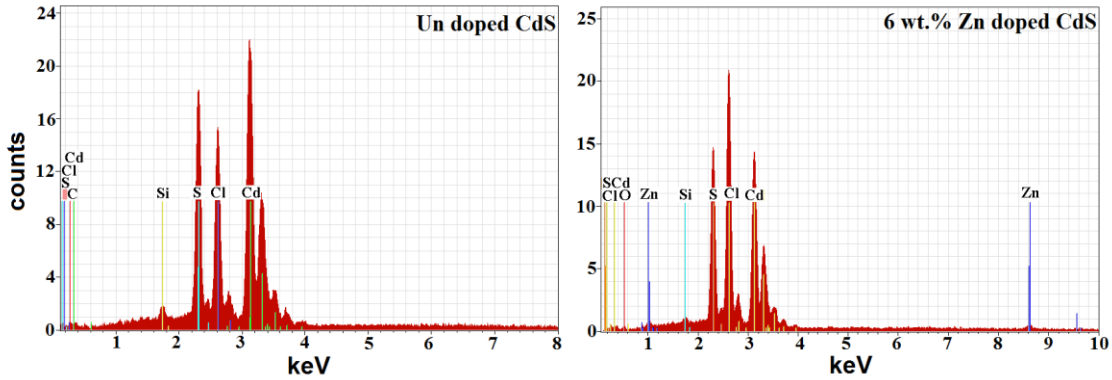

Figure 5: EDAX spectra of undoped and Zn-doped CdS (6 wt.% Zn concentration) thin films

The elements Cd, Zn and S are present in the doped sample and the other elements Si and Cl which are not expected in the films may be resulted from the glass substrate.

3.3 Optical studies

The optical properties of thin films such as transmission, refractive index and energy gap are of great importance to identify their suitability as window layer material for solar cell applications. The transmittance spectra of Zn-doped CdS thin films are shown in Figure 6. The transmittance increases with increasing Zn concentration. Undoped CdS sample showed a transmittance of about 78% in the visible region, which increased to 90% for the doped samples, which may be attributed to the lesser crystallite size of these films as observed from the XRD analysis (Table 2). It is well known that when the crystallite size is small, the smoothness of the film increases which cause an enhancement in the optical transmittance.

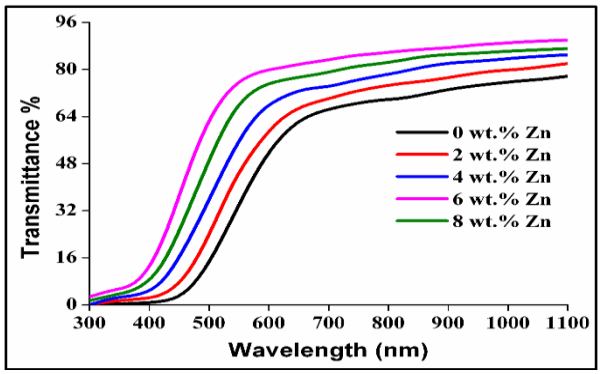

Figure 6: Transmittance spectra of CdZnS films.

The higher transmittance indicates lower defect density and better electrical properties of the doped CdS films because absorption of light in the longer wavelength region (>500 nm) is usually caused by crystalline defects such as grain boundaries and dislocations [18]. Furthermore, from the absorption spectra, the optical band gap energy E_g of the Zn-doped CdS thin films were calculated using the dependence of the absorption coefficient (α) on the photon energy (hυ) [19]:

$$\alpha h\upsilon = A\,(h\upsilon - E_g)^{\frac{1}{2}} \qquad (4)$$

Figure 7 shows the plot of $(\alpha h\upsilon)^2$ vs. (hυ) for the undoped and Zn-doped CdS thin films. Extrapolation of the linear portion of the plot onto the energy axis gives the band gap values of the films.

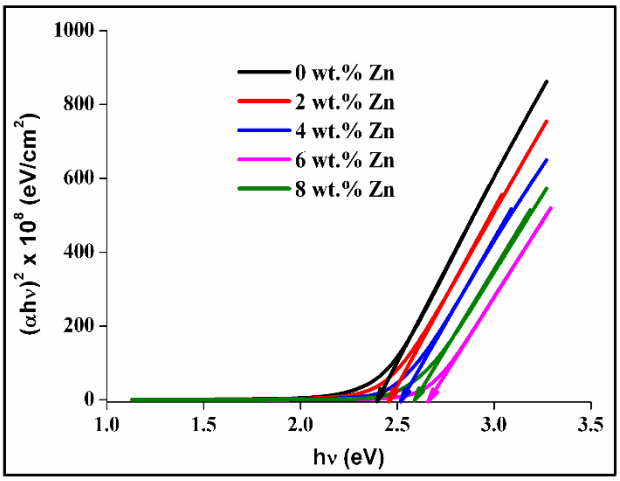

Figure 7: Plots of $(\alpha h\nu)^2$ vs. (hν) for the undoped and Zn-doped CdS thin films.

The E_g value of undoped CdS film is 2.4 eV. The band gap value obtained for the undoped film is in agreement with the value reported by Anbarasi et al [20] for CdS films fabricated by spray pyrolysis technique using perfume atomizer. The E_g value increases gradually as the Zn doping level increases and attains a maximum value of 2.66 eV for the CdS film doped with 6 wt.% Zn concentration. Beyond this doping concentration, the band gap decreases to 2.5 eV for the CdS film coated with 8 wt.% Zn concentration. This variation in E_g is associated with the Moss-Burstein (MB) effect or band gap widening (BGW) mechanism [21]. According to Moss – Burstein effect, the optical absorption edge of a degenerate n-type semiconductor is shifted towards higher energy by an amount proportional to the electron density in the conduction band. From theoretical calculations, Zaoui et al. [22] proposed that the optical band gap of Zn-doped CdO films increases if Zn^{2+} ions successfully replace Cd^{2+} ions in the CdO lattice. The increased band gap values observed here confirms that Zn^{2+} ions successfully replace Cd^{2+} ions in the CdS lattice. Increased band gap values observed for the CdZnS films might be due to decreased crystallite size values which lead to quantum confinement of the charge carriers in the crystallites and this result in the reduction of band bending effect, the degree of preferred orientation, and stoichiometry [23]. In nanocrystalline materials, band bending effect can be expected at the grain boundaries as the surface to volume ratio is higher.

Normally, in crystallites with smaller size, the band bending effect will be more compared to bigger crystallites. Owing to quantum confinement, the band gap increases due to reduced crystallite size, which result in the shift of absorption threshold to shorter wavelength due to individual confinement of electrons and holes. The energy gap broadening may also be related to the existence within the band gap of a high density levels with energies near the bands, which can give rise to band tailing as has been suggested for many polycrystalline materials. This is in accordance with the results reported by Rajashree et al. [24] for Cd-doped PbS thin films. The wide band gap and high optical transparency observed for the CdZnS films make them possible window layers in solar cell applications.

3.4 Electrical studies

Figure 8 shows the variation of resistivity of CdZnS films as a function of Zn concentration.

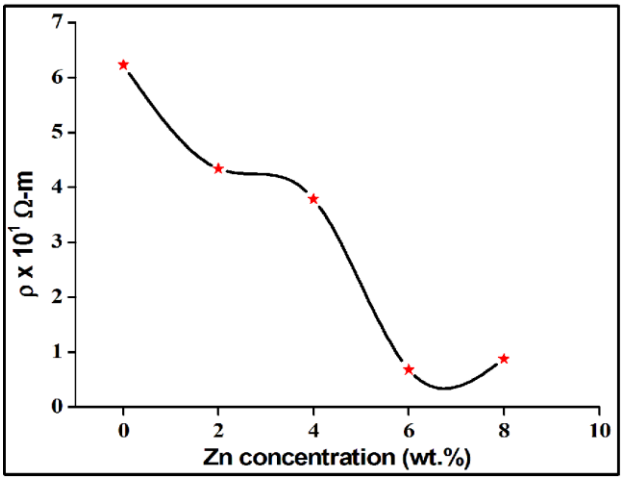

Figure 8: Variations of electrical resistivity of CdZns thin films as a function of Zn doping concentration.

As seen in Figure 8, the resistivity decreases with increasing Zn doping concentration in the films up to 6 wt.%, after which it slightly increases. The decreases in resistivity up to 6 wt % Zn concentrations might be due to the increase in the carrier concentration of the doped films due to the substitutional replacement of Cd^{2+} ions by Zn^{2+} ions. Flores et al [25] also reported a similar behaviour for fluorine doped CdS thin films. They quoted that the free carrier concentration increases due to substitutional

incorporation of F^- ions in the CdS structure which results in the decreased resistivity of the films. DeMelo et al [26] quoted sulphur deficiencies contribute to the increase in free carrier concentration of the films, which reduces the resistivity of the films. Although the crystalline quality of CdS film slightly decreases with Zn doping increased sulphur vacancies might have played an important role in improving its electrical properties.

3.5 PL studies

Photoluminescence (PL) is a process in which an electron, excited by monochromatic photon beam of certain energy undergoes radiative recombination either at valence band (band edge luminescence) or at traps/surface states (normally red shifted luminescence) within the forbidden gap [27]. The room temperature photoluminescence spectra of CdS and Zn-doped CdS (Zn doping level: 6wt. %) films excited at $\lambda = 230$ nm are presented in Figure 9.

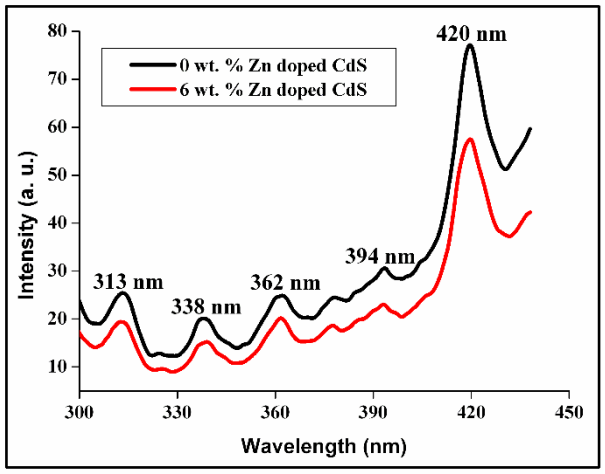

Figure 9: PL spectra of CdZnS thin films.

The samples exhibit emission peaks at 313, 338, 362, 394 and 420 nm respectively. The peak at 313 nm may be attributed to the transitions due to excitons at higher energy levels. The emission peak observed at 338 nm may be attributed to the transition due to excitons at higher energy levels. Maleki et al. [28] observed a similar peak at 340 nm in CdS nanoparticles which they assumed to be caused by recombination of excitons and/or shallowly trapped electron-hole pairs. The emission peak centred at 362 nm is ascribed to the ultraviolet emission to the recombination of free exciton [29]. The emission peak observed at 394 nm is due to the electron transition from the localized level slightly below the conduction band to the valence band [30]. S vacancy states are also responsible for this peak. The S vacancies act as deep level trap for electrons and they can exothermically extract electrons from the valence band [31]. Emission band at 420 nm can be ascribed to a high level transition in CdS semiconductor crystallites, which is usually related to the transition of electrons from the conduction band edge to holes, trapped at interstitial Cd^{2+} sites.

3.6 Raman studies

Figure 10 shows the Raman spectra of CdZnS thin films in the low frequency region 300-800 cm^{-1} which revealed two modes (1LO and 2LO) for both undoped and doped samples. It is well known that Raman scattering spectra can give useful information about the crystallinite quality of the film by evaluating the spectral peak position and the spectral width of the Raman spectra.

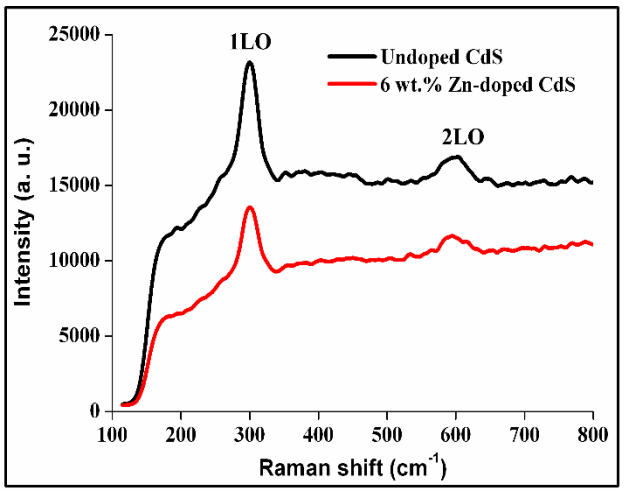

Figure 10: Raman spectra of CdZnS thin films.

For both hexagonal wurtzite and cubic zinc blende structured CdS, the zone center of the first order longitudinal optical (1LO) phonon frequency is about 305 cm^{-1} [32] and for the second order longitudinal optical (2LO) phonon frequency it is at about 600 cm^{-1}. It can be observed from Figure 5, the 1LO mode at 300 cm^{-1} dominates the spectra and the weak 2LO mode appears at 604 cm^{-1}. It is observed that the intensity of the Raman peaks changes due to the damage and disorder induced by Zn incorporation. Ozer et al. [33] reported that the intensity of Raman peaks of Sn-doped CdS thin films decreases due to the reduction of Sn vacancies in the films.

3.7 FTIR analysis

The FTIR spectra of undoped CdS and Zn-doped CdS film with 6 wt.% Zn concentration are shown in Figure 11.

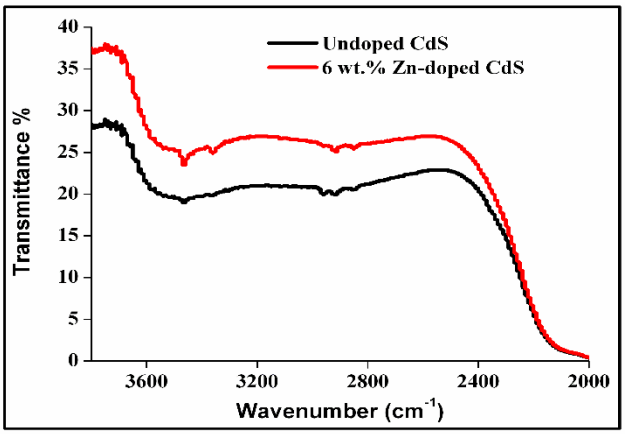

Figure 11: FTIR spectra of CdZnS thin films.

No significant difference between the spectra corresponding to doped and undoped film is observed. However, some bands of the FTIR spectra not observed in the undoped sample appears in the doped sample and also some bands are slightly shifted to lower values for the doped film which might be due to changes in the surface microstructures, residual stress, structural disorder and differences in grain size with very weak effect. The peaks of weak intensities observed at 2800-2900 cm^{-1} is attributed to C-H stretching vibrations [34] and these peaks fully correlate with the observed frequencies 2855 cm^{-1} and asymmetric stretches respectively [35]. The weak peak observed at 3580 cm^{-1} is attributed to hydrated water and the hydroxyl group which results from the hygroscopic nature of CdS [36].

4 Conclusion

CdZnS thin films with different Zn concentrations were fabricated on glass substrates by spray pyrolysis technique using a perfume atomizer. All the films showed hexagonal crystal structure with (0 0 2) preferential orientation. The diffraction peak (0 0 2) shifts towards higher 2θ value with increase in Zn concentration. The lattice parameter values decreases due to the replacement of cadmium by zinc atoms. Zn doping modified the surface morphology to a large extent. The band gap value of ZnCdS films increased from 2.4 eV to 2.66 eV with increasing Zn concentration. This blue shift in the band gap value is attributed to MB effect. Film resistivity decreased with increasing Zn concentration. The photoluminescence and Raman spectra were not affected significantly with Zn doping. The high transmittance, widened band gap and low resistivity obtained for CdZnS thin films make them promising candidate for optoelectronic devices as well as window layer in solar cell applications.

Acknowledgements

The authors are thankful to the Head, Department of Chemistry and Mr.Gowtham, Gandhigram Rural Institute, Dindugal for the SEM and EDAX measurements. The authors thank Mr. Karthik, Technical officer and Head, Department of Physics for the XRD, FTIR and Raman analysis.

References

[1] I.L. Oladeji, C. Chow, V. Ferekides, V. Viswanathan, Z. Zhao, Metal/CdTe/CdS/$Cd_{1-x}Zn_xS$/TCO/glass: A new CdTe thin film solar cell structure, Sol. Energy Mater. Sol. Cells, **61**(2000) 203–211.

[2] J.K. Dongre, M. Rarakhiani, J. Alloys Compnds. **487**(2009) 653

[3] H. Khallaf, I.O. Oladeji, L. Chow, Optimization of chemical bath deposited CdS thin films using nitrilotriacetic acid as a complexing agent, Thin Solid Films, **516**(2008) 5967–5973.

[4] X.Wu, High-efficiency polycrystalline CdTe thin-film soalr cells, Solar Energy, **77**(2004) 803–814.

[5] G. Perna, V. Capozzi, M. Ambrico, V. Augelli, T. Ligonzo, A. Minafra, L. Schiavulli, M. Pallara, Structural and optical characterization of undoped and indium-doped CdS films grown by pulsed laser deposition, Thin Solid Films, **453**(2004) 187–194.

[6] B. Patil, D. Naik, V.Shrivastava, Synthesis and characterization of Al doped CdS thin films grown by chemical bath deposition method and its application to remove dye by photocatalitic treatment, Chalcogenide Lett. **8**(2011) 117–121.

[7] H. Khallaf, G. Chai, O. Lupan, L. Chow, S. Park, A. Schuite, Characterization of Gallium-doped CdS thin films grown by chemical bath deposition , Appl.Surf. Sci. **255**(2009) 4129–4134.

[8] J. Lee, J. Yi, K. Yang, J. Park, R. Oh , Electrical and optical properties of boron doped CdS thin films prepared by chemical bath deposition Thin solid films, **432**(2003) 344–348.

[9] Q. Wang, Z. Xu, L. Yue, W.Ches, Opt . Master. **27**(2004) 453

[10] N. Badera, B. Godbole, S.B. Srivastava, P.N. Vishwakarm, L.S. Sharath Chandra , D. Jain, M. Gangrade, T. Shripathi, V.G.Sathe, V.G.sathe, V. Ganesan, Quenchig of photoconductivity in Fe doped CdS thin films prepared by spray pyrolysis technique, Appl.Surf. Sci. **254**(2008) 7042–7048.

[11] Hari Bala, Yanhui Yu, Xinxin CaO, Wuyou Fu, Preparation and characterization of nickel/zinc sulphide: Bifunctional magnetic-optical nanocomposites, Mater. Chem and Phy. **111**(2008) 50–53.

[12] M. Suganya, A.R. Balu, K. Usharani, Role of substrate temperature on the growth mechanism and physical properties of spray deposited lead oxide thin films, Mater. Sc.- Poland, **32**(2014) 448–456.

[13] T. Sivaraman, A.R. Balu, V.S. Nagarethinam, Effect of magnesium incorporation on the structural, morphological, optical and electrical properties of CdS thin films, Mater. Sci. Semicond. Proc. **27**(2014) 915–927.

[14] K. Usharani, N. Manjula, A.R. Balu, V.S. Nagarethinam, Mater. Res. Innovations, (2015 in press)

[15] A.R. Balu, V.S. Nagarethinam, M.G. Syed Basheer Ahamed, A. Thayumanavan, K.R. Murali, C. Sanjeeviraja, V. Swaminathan, M. Jayachandran, Influence of thickness on the microstructural, optoelectronic and morphological properties of nanocrystalline ZnSe thin films, Mater. Sci. Engg. B, **171**(2010) 93–98.

[16] N. Choudhury, B.K. Sarma, Structural characterization of lead sulphide thin iflms by means of X-ray line profile analysis, Bull. Mater. Sci. **32**(2009) 43–47.

[17] A.R. Balu, V.S. Nagarethinam, N. Arunkumar, M. Suganya, Nanocrystalline NiO thin films prepared by a low cost simplified spray technique using perfume atomizer, J. Electron Devices, **13**(2012) 920–930.

[18] M. Cao, L. Li, B.L. Zhang, J. Huang, H. Cao, Y. Sun, Y. Shen, Influence of substrates on the structural and optical properties of ammonia-free chemically deposited CdS films, J. Alloys Compnds. **530**(2012) 81–87.

[19] C. Rajashree, A.R. Balu, V.S. Nagarethinam, Substrate temperature effect on the properties of lead sulphide thin films suitable for solar control coatings, Int. J. ChemTech Res. **6**(2014) 347–360.

[20] M. Anbarasi, A.R. Balu, V.S. Nagarethinam, Comparative study of CdS thin films fabricated by a simplified spray technique using two cationic precursor salts with different stability constants, Int. J. Thin Film Sci. Technol. **3**(2014) 93–106.

[21] E. Burstein, Anomalous optical absorption limit in InSb, Physical Review **93**(1954) 632–633.

[22] A. Zaoui, M. Zaoui, S. Kacimi, A. Boukortt, B. Bouhafs, Stability and electronic properties of $Zn_xCd_{1-x}O$ alloys, Mater. Chem. Phys. **120**(2010) 98–103.

[23] J.P. Enriquez, X. Mathew, Influence of the thickness on structural, optical and electrical properties of chemical bath deposited CdS thin films, Sol. Energy Mater. Sol. Cells, **76**(2003) 313–322.

[24] C. Rajashree, A.R. Balu, V.S. Nagarethinam, Properties of Cd-doped PbS htinf films: Doping concentration effect, Surf. Engg. **31**(2015) 316–321.

[25] F.de Moure-Flores, K.E. Nieto-Zepeda, A. Guillen - Cervantes, S. Gallando, J.G. Quinones-Galvan, A. Hernandez- Hernandez, M.de la L.Olvera, M.Zapata-Torres, Yu Kundriavtsev, M.Melendez-Lira, Effect of the immersion in $CdCl_2$ and annealing on physical properties of CdS:F films grown by CBD, J. Phy. Chem. Solids, **74**(2013) 611–615.

[26] O. De Melo, L. Herandez, O. Zelaya-Angel, R. Lozada-Morales, M. Becerril, E. Vasco, Low resistivity cubic phase CdS films by chemical bath deposition technique, Appl-phys.Lett. **65**(1994) 1278–1280.

[27] T. Sivaraman, V.S. Nagarethinam, A.R. Balu, CdS thin films fabricated by a simplified spray technique from different substrate temperatures – Structural, morphological, optical and electrical analysis, Res. J. Mater. Sci. **2**(2014) 6–15.

[28] M. Maleki, M. Sasani Ghamsari, S.H. Mirdamadi, R. Ghasemzadeh, Template-based growth of TiO_2 nanorods by sol-gel process, Semicond. Phys. Quantum Electron. Optoelectron. **10**(2007) 36–39.

[29] N.B. Ibrahim, S.M. Al-Shomar, Sahrim Hj. Ahmed, Effect of aging time on the optical, structural and photoluminescence properties of nanocrystalline ZnO films prepared by sol-gel method, Appl. Surf. Sci. **283**(2013) 599–602.

[30] A.N. Mallika, A. Ramachandra Reddy, K. Sowribabu, Ch. Sujatha, K. Venugopal Reddy, Structural and photoluminescence properties of Mg substituted ZnO nanoparticles, Opt.Mater. **36**(2014) 879–884.

[31] N. Chestsoy, T.D. Harris, R. Hull, L.E. Brus, Luminescence and photophysics of CdS semiconductor clusters: The nature of the emitting electronic state, Phys. Chem. **90**(1986) 3933–3937.

[32] J. Lee, Raman scattering and photoluminescence analysis of B-doped CdS thin films, Thin solid films, **451**(2004) 170–174.

[33] Tuley ozer, Sabita Aksay, Salih Kose, Vibrational; and morphplogicl properties of Sn –doped CdS films deposited by ultrasonic spray pyrolysis method, Master. Sci. Semicond. Proe. **13**(2010) 325–328.

[34] H. Tang, M. Yan, H. Zhang, M. Xia, D. Yang, Preparation and characterization of water-soluble CdS nanocrystals by surface modification of ethylene diamine, Mater. Lett. **59**(2005) 1024–1027.

[35] NA. Li, X. Zhang, S. Chen, X. Hou, Synthesis and characterization of CdS nanoparticles in the presence of oleic acid as solvent and stabilizer, J. Phy. Chem. Solids, **72**(2011) 1195–1198.

[36] N.R. Yogamalar, A.C. Bose, Tuning the aspect ratio of hydrothermally grown ZnO by choice precursor, J. Solid State Chem. **184**(2011) 12–20.